MOLECULAR ONCOLOGY 9 (2015) 834–849

available at www.sciencedirect.com

ScienceDirect

www.elsevier.com/locate/molonc

Honokiol confers immunogenicity by dictating calreticulin exposure, activating ER stress and inhibiting epithelial-to-mesenchymal transition

Shing-Hwa Liu[a], Wen-Jane Lee[b], De-Wei Lai[c], Sheng-Mao Wu[c], Chia-Yu Liu[c], Hsing-Ru Tien[c], Chien-Shan Chiu[c,d], Yen-Chun Peng[e], Yee-Jee Jan[f], Te-Hsin Chao[g], Hung-Chuan Pan[h,i,1], Meei-Ling Sheu[b,c,j,*]

[a]Institute of Toxicology, College of Medicine, National Taiwan University, Taipei, Taiwan
[b]Department of Education and Research, Taichung Veterans General Hospital, Taichung, Taiwan
[c]Institute of Biomedical Sciences, National Chung Hsing University, Taichung, Taiwan
[d]Department of Dermatology, Taichung Veterans General Hospital, Taichung, Taiwan
[e]Division of Gastroenterology, Department of Internal Medicine, Taichung Veterans General Hospital, Taichung, Taiwan
[f]Department of Pathology and Laboratory Medicine, Taichung Veterans General Hospital, Taichung, Taiwan
[g]Division of Colorectal Surgery, Department of Surgery, Taichung Veterans General Hospital, Taichung, Taiwan
[h]Faculty of Medicine, School of Medicine, National Yang-Ming University, Taipei, Taiwan
[i]Department of Neurosurgery, Taichung Veterans General Hospital, Taichung, Taiwan
[j]Rong Hsing Research Center for Translational Medicine, National Chung Hsing University, Taichung, Taiwan

ARTICLE INFO

Article history:
Received 7 June 2014
Received in revised form
22 December 2014
Accepted 22 December 2014
Available online 6 January 2015

Keywords:
Calreticulin
Endoplasmic reticulum stress
Epithelial-to-mesenchymal transition
Immunogenic cell death
Carcinogenesis

ABSTRACT

Peritoneal dissemination is a major clinical obstacle in gastrointestinal cancer therapy, and it accounts for the majority of cancer-related mortality. Calreticulin (CRT) is over-expressed in gastric tumors and has been linked to poor prognosis. In this study, immunohistochemistry studies revealed that the up-regulation of CRT was associated with lymph node and distant metastasis in patients with gastric cancer specimens. CRT was significantly down-regulated in highly metastatic gastric cancer cell lines and metastatic animal by Honokiol-treated. Small RNA interference blocking CRT by siRNA-CRT was translocated to the cells in the early immunogenic response to Honokiol. Honokiol activated endoplasmic reticulum (ER) stress and down-regulated peroxisome proliferator-activated receptor-γ (PPARγ) activity resulting in PPARγ and CRT degradation through calpain-II activity, which could be reversed by siRNA-calpain-II. The Calpain-II/PPARγ/CRT axis and interaction evoked by Honokiol could be blocked by gene silencing or pharmacological agents. Both transforming growth factor (TGF)-β1 and N-methyl-N′-nitro-N-nitrosoguanidine (MNNG) induced cell migration, invasion and reciprocal down-regulation of epithelial marker E-cadherin, which could be abrogated by siRNA-CRT. Moreover, Honokiol significantly suppressed MNNG-induced gastrointestinal tumor growth and over-expression of

Abbreviations: CRT, calreticulin; PPARγ, peroxisome proliferator-activated receptor-γ; EMT, epithelial-to-mesenchymal transition; ICD, immunogenic cell death; TAMs, tumor-associated macrophages; TGF-β1, transforming growth factor-β1; DAMPs, damage-associated molecular patterns; MVD, microvessel density.

* *Corresponding author*. Institute of Biomedical Sciences, College of Life Sciences, National Chung Hsing University, 250, Kuo Kuang Road, Taichung 402, Taiwan. Tel.: +886 4 23592525x4402; fax: +886 4 22853469.
E-mail addresses: mlsheu@nchu.edu.tw, mlsheu@vghtc.gov.tw (M.-L. Sheu).

[1] H.C.P contributed equally to first author.

http://dx.doi.org/10.1016/j.molonc.2014.12.009

CRT in mice. Knockdown CRT in gastric cancer cells was found to effectively reduce growth ability and metastasis *in vivo*. The present study provides insight into the specific biological behavior of CRT in epithelial-to-mesenchymal transition (EMT) and metastasis. Taken together, our results suggest that the therapeutic inhibition of CRT by Honokiol suppresses both gastric tumor growth and peritoneal dissemination by dictating early translocation of CRT in immunogenic cell death, activating ER stress, and blocking EMT.

1. Introduction

In cancer, peritoneal dissemination is the primary cause of metastasis from malignancies, which is associated with loss of epithelial characteristics and acquisition of a mesenchymal phenotype, initiating invasion and metastasis (De and Berx, 2013; Gherardi et al., 2012). Gastric cancer (GC) is the second leading cause for cancer-related death world and the majority of patients will relapse after definitive surgery. Additionally, GC patients exhibit a high incidence of lymph node metastases. Thus, the overall 5-year survival rate in GC patients remains poor and there has been no significant improvement in the past decades (Lim et al., 2005). The major cause of death and relapse is generation of distant metastasis, which places considerable limits on the success of therapeutic modalities. Our recent reports have shown a close relationship between epithelial-to-mesenchymal transition (EMT) and gastric cancer progression (Pan et al., 2013a). EMT is a key process in the metastatic step that confers certain fundamental abilities in tumor cells migration, invasiveness and anoikis resistance. EMT and metastasis are controlled by distinct signaling molecules present in the tumor microenvironment such as transforming growth factor-β1 (TGF-β1), tumor necrosis factor-α, hepatocyte growth factor, inflammatory cytokine and a variety carcinogen such as N-methyl-N′-nitro-N-nitrosoguanidine (MNNG) (Pan et al., 2013a). EMT can be disrupted by numerous signaling pathways and regulatory transcriptional networks. Furthermore, post-transcriptional regulatory networks regulate EMT progression. Several signaling cascades, including developmental transcriptional factors, are involved in promoting tumor metastasis. Indeed, over-expression of transcriptional factors evokes the motile-invasion phenotype potential in human cancer. Of particular note, Snail overexpression (≥75% positivity) is associated with lymph node metastasis and poor prognosis, and is significantly correlated with overall survival among 314 GC patients (Shin et al., 2012). However, the precise molecular mechanisms that promote EMT and tumor dissemination in GC cells remain unknown.

Calreticulin (CRT), a Ca^{2+}-binding protein of the muscle sarcoplasmic reticulum in the lumen of the endoplasmic reticulum, has a variety of important biological functions involving intracellular Ca^{2+} homeostasis, regulation of Ca^{2+} signaling, modulation of gene expression, chaperoning, and cellular adhesion (Raghavan et al., 2013). The over-expression of CRT found in various diseases characterized by pathophysiological progressions such as systemic lupus erythematosus, rheumatic disease, and parasitic diseases including onchocerciasis has been reported (Eggleton and Llewellyn, 1999). However, emerging evidence has demonstrated that in tumor cells-treated by anthracyclines or γ-irradiation induced immunogenic cell death intracellular CRT (endo-CRT) is translocated to the plasma membrane surface (ecto-CRT), promoting tumor cell recognition and phagocytic uptake by immune cell-mediated elimination of the tumor (Chao et al., 2012; Eggleton and Llewellyn, 1999; Krysko et al., 2012; Raghavan et al., 2013; Zamanian et al., 2013). Ecto-CRT, an "eat me" signal in apoptosis, is thought to affect antigen presentation, complement activation, facilitate clearance of apoptotic cells, and enhance the immunogenicity of cancer cell death. Importantly, CRT is over-expressed in different types of malignancies like gastric cancer, colon cancer, and bladder cancer (Chen et al., 2009a, 2009b; Lu et al., 2011; Obeid et al., 2007). In addition, administration of exogenous CRT or pharmacological inhibitors of phosphatase 1/GADD34 revived the immunogenicity of cell death evoked by etoposide or mitomycin C, and improved their antitumor effects *in vivo* (Obeid et al., 2007). Indeed, correlations between the expression of CRT and the clinicopathological factors suggest that CRT could have valued a prognostic marker and served as an angiogenic regulator in human gastric cancer, which is in line with the associations of CRT with microvessel density (MVD), tumor invasion, lymph node metastasis, and survival (Chen et al., 2009a, 2009b). Previous reports have shown that suppression of tumor growth and metastasis in J82 human bladder cancer cells occurred by down-regulation of CRT expression via phosphorylation of FAK and paxillin (Lu et al., 2011). Conversely, there is strong evidence that CRT inhibits growth and/or metastasis of prostate cancer cells and that this suppression requires the P-domain (Alur et al., 2009). These results indicate that the function of CRT might play a pivotal role in cancer progression. However, the mechanism underlying CRT on EMT and cancer peritoneal dissemination remains unknown. Thus, there is a need to better understand the clinical and pathophysiological processes involved in tumor destruction by pharmacological intervention.

Honokiol is a small-molecule polyphenol isolated from the genus *Magnolia*, which has been shown to be a potential anticancer agent in various cancer models such as gastric, breast, colon, and prostate cancer (Fried and Arbiser, 2009). Intravenous injection of 5–10 mg/kg Honokiol showed the half-lives of disposition in rat plasma samples were 49.22 ± 6.68 and 56.24 ± 7.30 min. Meanwhile, intraperitoneal injection 250 mg/kg yielded a $t_{1/2}$ of 4–6 h, with a t_{max} of about 20–30 min in mice (Tsai et al., 1994). Our previous reports have shown that Honokiol activates apoptosis and inhibits tumorigenesis as well as metastasis of gastric cancer cells by

targeting the key endoplasmic reticulum (ER) stress pathways such as calpain activation, and down-regulation of peroxisome proliferator-activated receptor-γ (PPARγ), Grp94, COX-2, STAT-3 and Tpl-2 proteins (Lee et al., 2013; Liu et al., 2010a, 2012a; Pan et al., 2013a; Sheu et al., 2007). However, the anti-EMT potential of Honokiol and its enhancement of immunogenicity of cancer cell death have not been investigated in any cancer model. The present study was designed to elucidate the role of Honokiol in EMT and immunogenicity in gastric cancer.

2. Materials and methods

2.1. Materials

Most of the materials and methods listed here have been published previously but are presented here for clarity (Lee et al., 2013; Liu et al., 2010a, 2012; Pan et al., 2013a). Honokiol was obtained from Wako Chemical Company (Osaka, Japan).

2.2. Cell culture

Human gastric cancer cell lines: AGS and N87 (moderately differentiated gastric adenocarcinoma) and MKN45 and SCM-1 cells (poorly differentiated gastric adenocarcinoma) were obtained from the cell bank of Taipei Veterans General Hospital (Taiwan). Cells were grown in RPMI medium. Media were supplemented with 10% fetal bovine serum, 100 U/ml penicillin, and 100 μg/ml streptomycin (complete medium) at 37 °C in humidified incubator with 5% CO_2.

2.3. Tissue samples and clinical data collection

A total of 40 patients were analyzed in this study. After approval from the Taichung Veterans General Hospital institutional review board (CE12060), data from the cancer registry of the Cancer Institute of Tissue Bank was obtained. Information which was obtained through participating cancer registry included: age, gender, differentiation, tumor location, tumor size, depth of tumor invasion (T stage, according to the seventh edition UICC TNM classification for gastric cancer), number of metastatic lymph nodes (N stage, according to the seventh edition UICC TNM classification for gastric cancer), extent of lymph node metastasis, Lauren classification. The correlations between CRT expression and clinicopathological characteristics of gastric cancer patients were summarized in Table 1. For histology analysis of tumor stage, tumor grade and distant metastasis, Fisher's exact test was used. For comparison of clinicopathological characteristics, one-way analysis of variance was used. A p value of $p < 0.05$ was considered statistically significant.

2.4. Immunohistochemistry

Paraffin-embedded human gastric cancer tissues were obtained from the Taichung Veterans General Hospital Tissue Bank, and 5-μm sections were stained for CRT using the anti-CRT antibody as described in Table 2 (Lee et al., 2013; Liu et al., 2012; Pan et al., 2013a). Carcinogen MNNG-induced tumor growth or peritoneal dissemination model tumors were analyzed by immunohistochemical studies performed on 5-μm sections using PCNA and CRT antibodies (Santa Cruz Biotechnology).

Table 1 – Correlation between CRT expression and clinicopathological characteristics of gastric cancer.

Characteristics	Case (N = 40)	CRT expression		P-value*
		Low (N = 13)	High (N = 27)	
Gender				0.501
Male	26	9	17	
Female	14	4	10	
Age (years)				
Mean	40	62.3	66.9	0.628
Differentiation				0.633
Well	8	3	5	
Moderately	14	6	10	
Poorly	18	4	12	
Lauren classification				0.529
Intestinal	18	5	13	
Diffuse	22	8	14	
T classification				**0.038**
T1	3	1	2	
T2	5	2	3	
T3	18	6	12	
T4	14	4	10	
N classification				**0.032**
N0	10	5	5	
N1	14	4	10	
N2	12	3	9	
N3	4	1	3	
Distant metastasis				**0.039**
Negative	26	11	15	
Positive	14	2	12	
TNM stage				**0.035**
I	4	2	2	
II	10	3	7	
III	12	4	8	
IV	14	4	10	

Abbreviations: CRT = Calreticulin; TNM = tumor-node-metastasis. CRT staining of tissues was correlated with clinicopathological parameters including AJCC tumor staining manual 7th edition. Samples with incomplete patient data were excluded from some of the individual's analyses.

* The p-values were calculated by one-way analysis of variance, and by Fisher's exact test for the other parameters. Significant p-values are indicated in bold.

2.5. Immunofluorescence and laser scanning confocal microscopy

Cells were prepared and the immunofluorescence was determined by laser scanning confocal microscopy (LSCM, TCS SL, Leica, Wetzlar, Germany) as previously described (Liu et al., 2010b, 2012). Images (total magnification 400×) were background-subtracted and merged using the Confocal Assistant MetaMorph software program. Capture image from laser scanning confocal microscopy and organize data, and then redo the page layouts by Adobe Photoshop software.

Table 2 – Additional antibodies used in the study.

Name	Sp. (Clone number or code number)		In the work usage	Vendor
Primary antibody				
Calreticulin	sc-11398	rabbit polyclonal IgG	WB,IF	Santa Cruz Biotechnology
CD47	sc-12730	mouse monoclonal IgG	WB,IF	Santa Cruz Biotechnology
Calpain I	sc-7531	goat polyclonal IgG	WB	Santa Cruz Biotechnology
Calpain II	sc-7533	goat polyclonal IgG	WB	Santa Cruz Biotechnology
PDI	sc-20132	rabbit polyclonal IgG	WB	Santa Cruz Biotechnology
GAPDH	sc-32233	mouse monoclonal IgG	WB	Santa Cruz Biotechnology
PPARγ	sc-7273	mouse monoclonal IgG	WB	Cell Signaling
E-cadherin	sc-7870	rabbit polyclonal antibody	WB,IHC(P)	Santa Cruz Biotechnology
E-cadherin	3195	monoclonal antibody	WB	Cell Signaling
Snail	sc-28199	rabbit polyclonal IgG	WB,IHC(P)	Santa Cruz Biotechnology
PCNA	sc-56	mouse monoclonal IgG	WB,IHC(P)	Santa Cruz Biotechnology
Pecam1(CD31)	sc-8306	rabbit polyclonal IgG	WB,IHC(P)	Santa Cruz Biotechnology
Hoechst	H3570		IF	Invitrogen
Secondary antibody				
Fluorescein-Labeled Antibody To Rabbit IgG (H+L)	02-15-16		IF	Kirkegaard & Perry Laboratories, Inc.
Doenkey anti-goat HRP	sc-2020		WB	Kirkegaard & Perry Laboratories, Inc.
Peroxidase-conjugated AffiniPure goat anti-mouse IgG (H+L)	115-035-003		WB	Jackson ImmunoResearch Laboratories, Inc.
Peroxidase-conjugated AffiniPure goat anti-rabbit IgG (H+L)	111-035-003		WB	Jackson ImmunoResearch Laboratories, Inc.
Rhodamine-Labeled Affinity Purified Antibody To Mouse IgG (H+L)	03-18-06		IF	Kirkegaard & Perry Laboratories, Inc.
Rhodamine-Labeled Affinity Purified Antibody To Rabbit IgG (H+L)	03-15-06		IF	Kirkegaard & Perry Laboratories, Inc.
Fluorescein-Labeled Antibody To Mouse IgG (H+L)	172-1806		IF	Kirkegaard & Perry Laboratories, Inc.

WB: Western blot; IF: immunofluorescence; IHC(P): immunohistochemistry (paraffin)

2.6. *Immunoblotting*

Immunoblotting was performed as described previously (Lee et al., 2013; Liu et al., 2010a, 2012; Pan et al., 2013a). Whole cell lysate proteins (60 μg) were separated by SDS-PAGE and electrophoretically transferred to nitrocellulose membranes. After blocking, the blots were incubated with antibodies overnight. Membranes were then incubated for 1 h with secondary antibody. Detection was performed by ECL (Amersham) and by chemiluminescence using Kodak X-Omat film. The antibodies used in this study were listed in Table 2.

2.7. *Time-lapse monitoring of cancer cells phagocytosis by macrophages* in vitro

Gastric tumor cells MKN45 were seeded onto Lab-Tek Permanox (Thermo Scientific-Nunc) chamber slides and labeled with 20 μM CFSE, then incubated with Honokiol for 2–4 or 16–20 h. Human THP-1 leukemia cells were labeled with CellTrace™ Calcein Red-Orange, and following exposure to phorbol-12-myristate-13-acetate (PMA, 300 nM) the cells were allowed to adhere for 30 min, then were added to each respective chamber. Phagocytosis was imaged using a BioStation IMQ (Nikon) equilibrated to 37 °C and 5% carbon dioxide. Images were captured at 2-min intervals and movies were made using the BioStation IM version 2.12 software at a rate of three frames per second.

2.8. *Transfection*

Cancer cells AGS and MKN45 were transfected with 1 μM siRNA-CRT, siRNA-PPARγ, siRNA-calpain-II (Santa Cruz Biotechnology) or 2 μg/ml shRNA-CRT (National RNAi Core Facility Platform, Taipei, Taiwan), or CRT-overexpressed plasmid 1 μg/ml pcDNA-CRT (Genome Research Center, National Yang-Ming University) using Lipofectin reagent (Invitrogen) according to the manufacturer's instructions.

2.9. *Luciferase reporter assay*

Cells at 60% confluence were co-transfected with 0.2 μg of the promoter reporter construct PPRE, and 0.1 μg of a thymidine kinase promoter driven Renilla-luciferase vector (pRLTK; Promega, Mannheim, Germany). After incubation, cells were lysed and processed using the Dual Luciferase Kit (Promega) as described by the manufacturer. Luciferase activity was normalized to Renilla firefly activity for transfection efficiency and recorded by a luminometer (LKB, Rockville, MD).

2.10. *ER stress response element (ERSE)*

Cignal ERSE Reporter Assay Kit was performed as described in accordance with the manufacturer's instructions (QIAGEN) using dilute transfection-ready reporter, negative control, positive control formulations and relevant test nucleic acids (siRNA, shRNA). Post-transfection overnight, transfected cells

were treated with Honokiol and ER stress activator. The activities of the signaling pathways were then assayed using dual luciferase assay.

2.11. Electrophoretic mobility shift assay (EMSA)

The electrophoretic mobility shift assay was performed as described previously (Liu et al., 2010a,b, 2012; Pan et al., 2013b). The consensus sequence-specific oligonucleotide probes were end-labeled according to the manufacturer's recommendations. The oligonucleotide with the PPARγ consensus binding sequence was used (PPARγ/CRT, 5′-GGTAAAATTGATTATCTCAAGGTCAGAAGC-3′). For the binding reaction, 2 ng labeled oligonucleotide and 2 μg poly dIdC (Amersham Pharmacia Biotech) carrier were incubated with 2 μg nuclear protein in a binding buffer (10 mM HEPES, 60 mM KCl, 1 mM DTT, 1 mM EDTA, 7% glycerol, and pH 7.6) for 30 min at room temperature. DNA–protein complexes were resolved on 6% non-denaturing polyacrylamide gels and visualized by exposure to auto-radiographic films.

2.12. Chromatin immunoprecipitation assay (ChIP)

The ChIP assay protocol was performed as described previously (Lai et al., 2014). Briefly, cells were fixed with formaldehyde, and were then homogenized and sonicated. The resulting supernatant was divided into aliquots for 10-fold dilution in ChIP dilution buffer and pre-cleared with protein A–Sepharose that contained salmon sperm DNA for 1 h. The antibodies were added and incubated for 12–18 h at 4 °C, and the complexes were collected with 50% slurry of protein A–Sepharose for 3 h. The beads were washed, and chromatin complexes were eluted from the beads. After performing reversal of cross-linking, DNA was purified, and 4 μl of input control or ChIP samples were used as a template in PCR using the primer sets for region. In the experiments using cells, 1 μl 1×10^6 cells were fixed with formaldehyde, harvested, and then sonicated as described above. A fragment of the (260 bp) Snail promoter contained putative PPARγ-binding sites. The primer used was 5′-GGAGTGTGTACCGCCATCTT-3′. The PPARγ consensus binding sequence binding to the CRT promoter was predicted *in silico by* Transcriptional Regulatory Element Database and double confirmed by NCBI data base.

2.13. In vitro proteolysis of PPAR-γ or CRT by calpain

Cleavage of PPAR-γ or CRT by calpain-2 was analyzed by a modified procedure as described previously (Pan et al., 2013a,b).

2.14. Invasion assay

Transfection with siRNA-CRT or CRT overexpressed plasmid to AGS or MKN45 cells was measured as reported previously, with some modification (Lee et al., 2013; Pan et al., 2013a). Briefly, 5×10^4 cells were suspended in 500 μl of serum-free medium in the absence or presence of Honokiol and placed onto the upper compartment of Matrigel-coated polycarbonate filters (Transwell, BD Biosciences; 8 μm pore size). The lower compartment was filled with 500 μl of medium containing 5% FBS in the absence or presence of Honokiol. After 20 h, cells on the upper surface of the filter were carefully removed with a cotton swab, and the membranes were fixed in methanol and stained with crystal violet. The cells that had migrated through the membrane to the lower surface of the filter were counted using a microscope.

2.15. Animal model

All animal care and experimental procedures were approved and conducted by the Committee for Animal Experiments of National Chung Hsing University (Approval Document NCHU-100-26). In carcinogenesis assay, male and female BALB/c and C57BL/6 mice, 4–6 weeks old were used. Mice were injected intraperitoneally with MNNG (5 mg/kg, twice/weekly, i.p.) for 1, 3, and 6 months. In some experiments, mice were injected with MNNG for 3 months and then divided into the control and Honokiol-treated (5 mg/kg, twice/weekly, i.p.) groups for 3 months. The body organs were examined for tumor growth, and various tissues were processed for histological examination. The peritoneal dissemination assay was conducted as previously described. Transfections of siRNA-CRT or shRNA-CRT (data not shown) into MKN45 cancer cells were performed using Lipofectin. The MKN45 siRNA CRT (1×10^6) cells were transected for 24 h and then each of the mice received one of the cell types via intraperitoneal injection to the abdominal cavity for 30 days. Quantification of the tumor mass was evaluated by one slide section and vessels were estimated by counting five randomly chosen high-power fields.

2.16. Statistical analyses

The study statistical analyses were performed with SAS software (SAS Institute, Cary, N.C.). The values were presented as mean ± SEM. Analysis of variance, followed by Fisher's least significant difference test, was performed for all data. Statistical significance was set at $p < 0.05$.

3. Results

3.1. Up-regulation of CRT in gastric tissues and gastric cancer cell lines and Honokiol triggers early surface exposure of CRT in immunogenic cell death and later down-regulation of CRT

Comparative evaluation of 40 paired gastric cancer tissues by immunohistochemical staining analysis, with each compared with benign tissue adjacent to the tumor from the same patient, showed that the CRT protein level was higher in all gastric cancer samples compared with their corresponding begin adjacent tissues (Figure 1A). The percentage of positive tumor cells and the staining intensity for each sample were recorded. A significant statistical difference was found between the positive expression rate of the CRT in tumor tissues and para-neoplastic tissues in two groups (Table 1). The level of CRT expression was closely correlated with gastric cancer clinical staging as well as clinical classification and distant

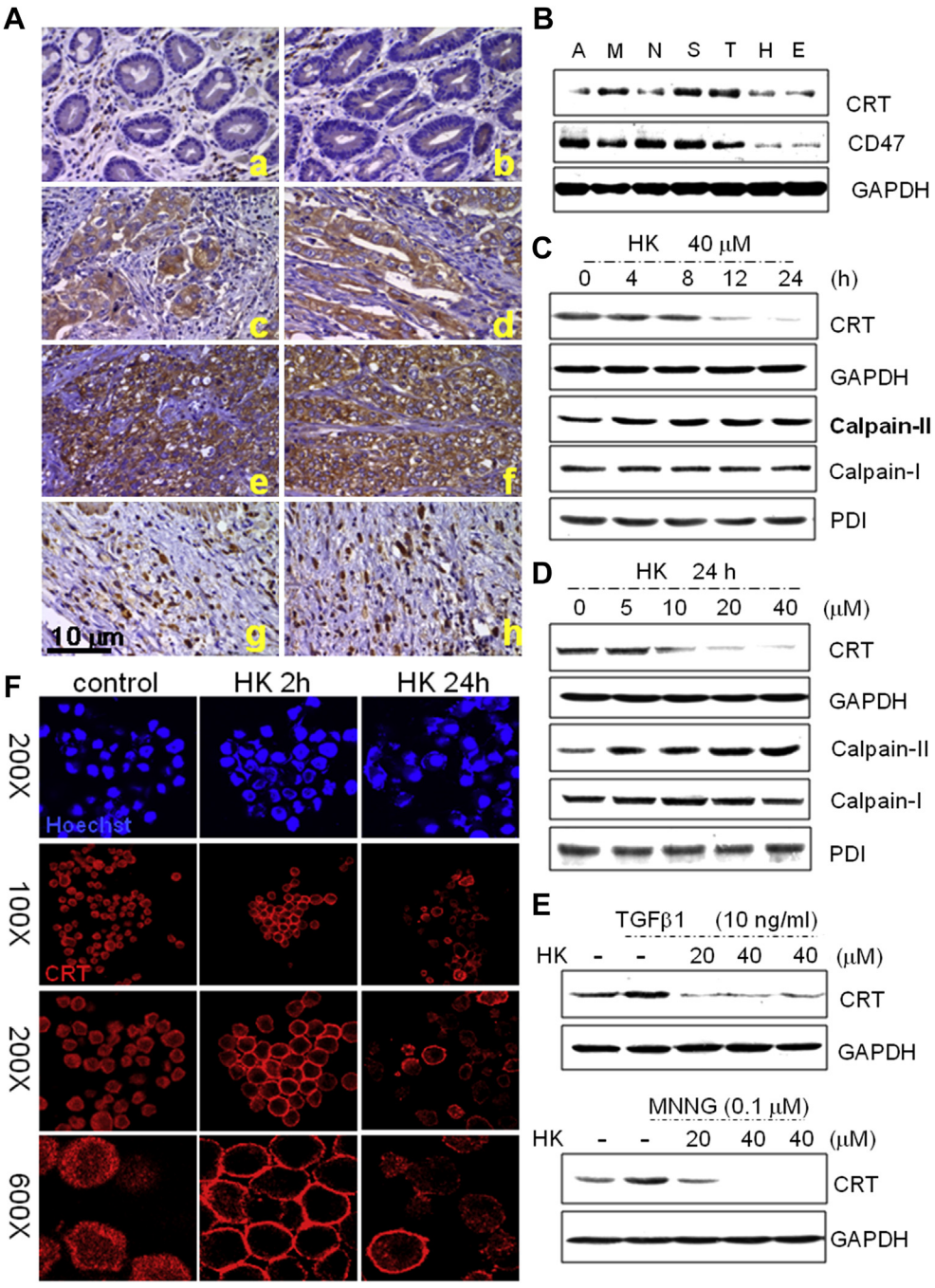

Figure 1 – Calreticulin (CRT) expression in gastric tissues and Honokiol trigger early surface exposure of CRT in immunogenic cell death, lately down-regulation of CRT. (A) a–b. Representative immunohistochemical staining of CRT expression in a human normal gastric mucosa. c–d. Moderately differentiated intestinal type adenocarcinoma. e–f. Poorly differentiated intestinal type adenocarcinoma. g–h. Diffused type adenocarcinoma in mucosa. Scale bar: 10 μm. (B) CRT protein expression differed in various gastric cancer cell lines AGS (A), MKN45 (M), N87 (N), and SCM-1 (S), mouse tumors mass (T), primary human endothelial cells (HUVECs, H), and primary mouse gastric epithelial cells (E). (C–D) Western blot analyses for CRT in MKN45 cells treated with Honokiol for time–response manner and dose–response manner. (E) Cancer cells were pretreated with Honokiol followed by stimulation with Transforming growth factor-β1 (TGF-β1) or N-methyl-N′-nitro-N-nitrosoguanidine (MNNG) for 24 h. The results shown are representative of at least four independent experiments. HK, Honokiol. (F) Confocal microscope image for translocation of CRT in MKN45 cells treated with Honokiol for time-course dependent. Cells were fixed on glass coverslips and labeled with Hoechst 33342 to stain nuclei and Texas red conjugated secondary antibody to anti-CRT primary antibody (*red*).

metastasis of in Tumor-Node-Metastasis classification, respectively. Furthermore, protein level CRT expression differed in various gastric cancer cell lines AGS (A), MKN45 (M), N87 (N) and SCM-1 (S), mouse tumor mass (T), primary human endothelial cells (HUVECs, H) and primary mouse gastric epithelial cells (E) shown in Figure 1B. Highly invasive cells MKN45 expressed higher CRT. Normal cells lower CRT expression pattern. We then examined whether CRT down-regulation

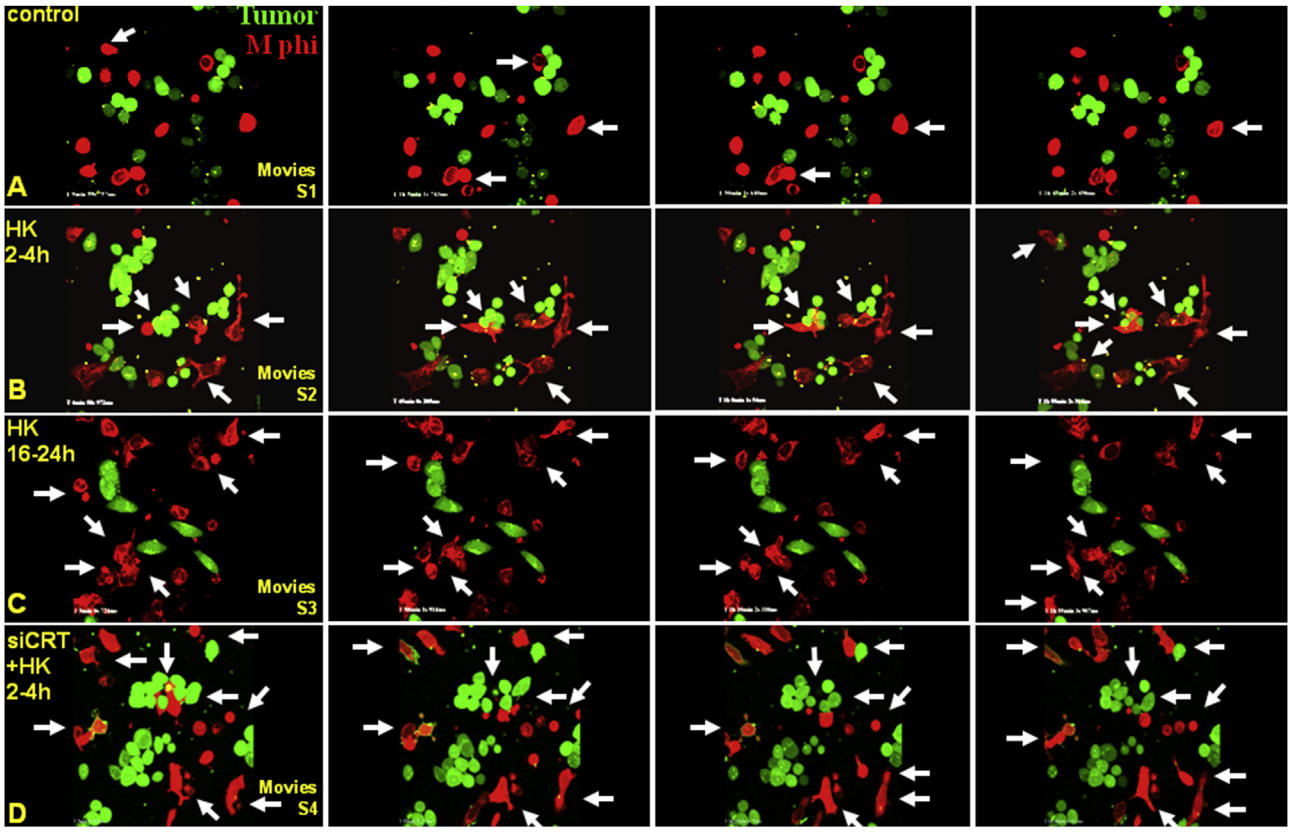

Figure 2 – Real-time monitoring of MKN45 cell phagocytosis by macrophages. Red florescence label positive THP-1 macrophages (red) and fluorescently labeled MKN45 gastric cancer cells (green) were co-cultured in the presence of control (A), Honokiol-treated 2–4 h (B), Honokiol-treated 16–24 h (C) or silencing CRT (D) and were imaged using video microscopy. (Movies S1, control; S2, Honokiol-treated 4 h; S3, Honokiol-treated 18 h and S4, transfection si-CRT+ Honokiol-treated 4 h). These time-lapse movie images showed the dynamic properties of cell–cell interaction as indicated by arrows. Results shown are representative of at least six independent experiments.

was controlled by Honokiol. In addition, we investigated whether Honokiol reduced tumorigenesis inducer TGFβ or carcinogenesis inducer MNNG induced CRT production. We found that Honokiol significantly down-regulated CRT, and up-regulated calpain-II expression but not calpain-I in a time-course and dose-dependent manner (Figure 1C–D). Honokiol was also shown to suppress TGFβ or MNNG-induced CRT (Figure 1E). Furthermore, we investigated whether stimulation with Honokiol inhibited expression of CRT. Unexpectedly, we found that Honokiol triggered early surface exposure of CRT to cell membrane in 2–8 h, followed later by down-regulation of CRT (Figure 1F) at 12–24 h by confocal microscopy detection. Therefore, Honokiol is unique in its ability to reduce CRT via a classic ER stress–calpain-II activation mechanism thereby enhancing early immunogenic response.

3.2. *Honokiol promotes early phagocytosis by dictating CRT exposure*

In experimental models of gastric cancer cells, ecto-CRT translocated to plasma membrane surface and mediated immunogenic cell death signaling by Honokiol induced phagocytosis of tumor cells and THP-1 macrophages. Given the hypothesis association of TAMs in MKN45 and the confirmation that Honokiol probably exerts therapeutic effects, we developed an *in vitro* assay to study the interaction between tumor cells and macrophages based on the hypothesis that Honokiol may enhance immunogenicity and enable phagocytosis of MKN45 cells by macrophages. To observe the interaction in real-time using live-cell imaging, red fluorescent dye label with macrophage-positive macrophages were derived using phorbol myristate acetate (PMA)-induced cell differentiation model of the human monocytic cell line THP-1 and MKN45 tumor cells were incubated with green fluorescently labeled MKN45 cells, which had been treated with Honokiol or parallel treatment with silencing of CRT transfection. Consistent with the results (Figure 1F) observed with human macrophages, the red fluorescent mouse macrophages were able to efficiently perform phagocytosis in Honokiol-treated cells in 2–4 h, in contrast to PBS- or DMSO-treated control cells (data not shown), which were not phagocytosed by the macrophages. Following ecto-CRT down-regulation, in which Honokiol treatment at 16–24 h retarded the phagocytosis effect. As expected, gene silencing targeting CRT abolished the immunogenic cell death (Figure 2

and Movies S1, S2, S3, S4). These time-lapse movies show that the cells–cells interaction dynamic properties of the arrows as indicated. These data provide strong evidence that Honokiol promote early phagocytosis by dictating CRT exposure.

Supplementary movies related to this article can be found online at http://dx.doi.org/10.1016/j.molonc.2014.12.009.

3.3. *Honokiol induces ER stress via calpain-II activation, which control PPARγ and CRT expression*

Calpain activation is a critical step during the ER stress response (Kepp et al., 2013; Krysko et al., 2012; Liu et al., 2010b, 2012; Pan et al., 2013a,b; Sheu et al., 2007). In order to

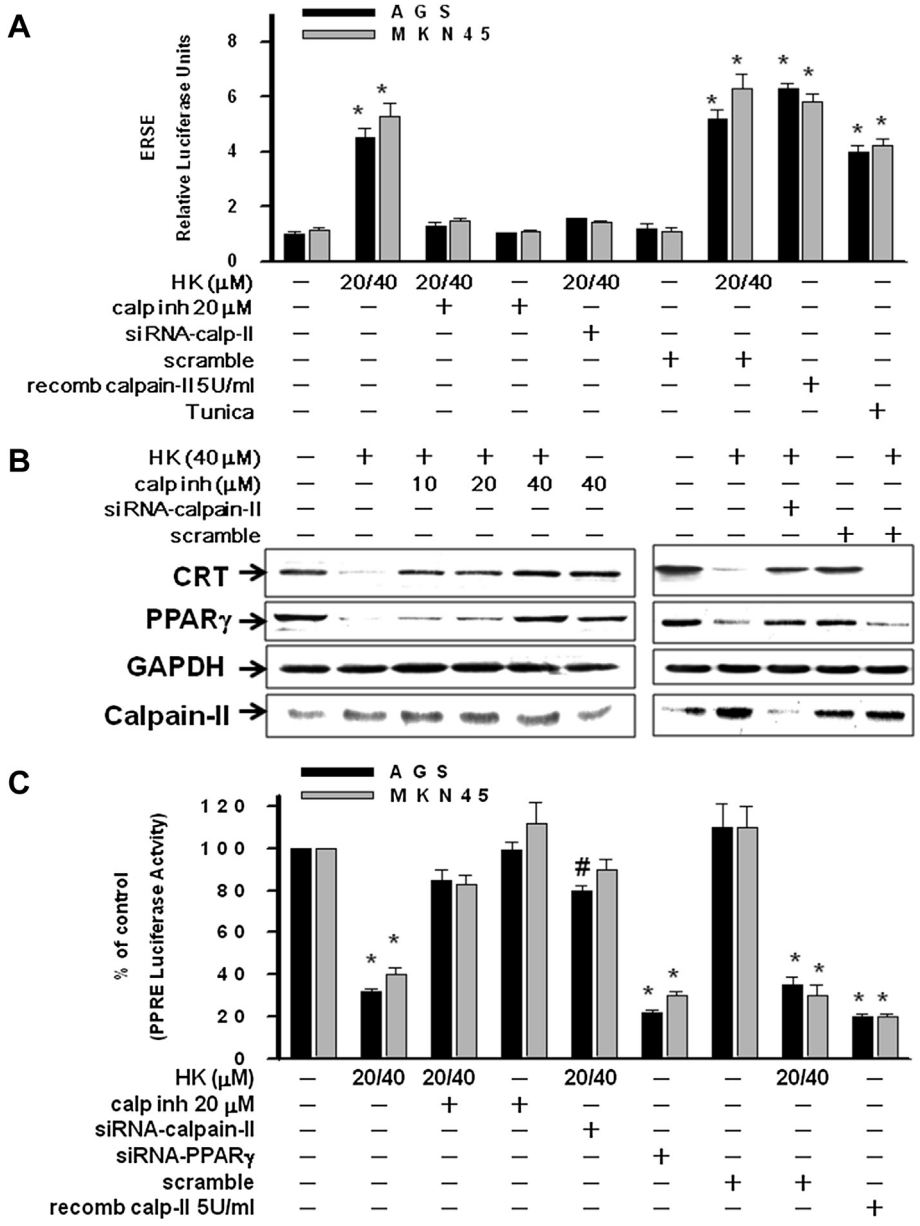

Figure 3 – Honokiol-induced calpain activation, cleavage PPAR-γ expression regulates CRT production. (A) ER stress activity by ERSE reporter detection. ERSE reporter is designed to measure activity of endoplasmic reticulum (ER) stress signaling. Cancer cells AGS or MKN45 were transfected with ERSE reporter, negative control and positive control (for transfection protocol refers our user material methods). Cancer cells were pre-incubated with calpain inhibitors, Honokiol, or transfected with siRNA-Calpain-II or scramble siRNA for 18 h, and the treated with Honokiol. Tunicamycin (0.1 μg/ml) taken as the positive control. Dual Luciferase assay was performed 36 h after transfection, and promoter activity values are expressed as arbitrary units using a Renilla reporter for internal normalization. Experiments were done in triplicates, and the standard deviation is indicated. (B) Cancer was pre-treated with calpain inhibitor or transfected with siRNA-Calpain-II or scrambled siRNA followed by stimulation with Honokiol for 24 h. Data shown are representative of at least three independent experiments. (C) Cancer cells that were transiently transfected with the PPRE luciferase reporter plasmid and a thymidine kinase promoter-driven Renilla-luciferase vector were transiently transfected with siRNA-Calpain-II, or siRNA-PPARγ or control scrambled RNA and treated with Honokiol. The relative activity was measured by luciferase assay as described in the Materials and methods section. Means ± SEM of luciferase activities were calculated from triplicate determinations.

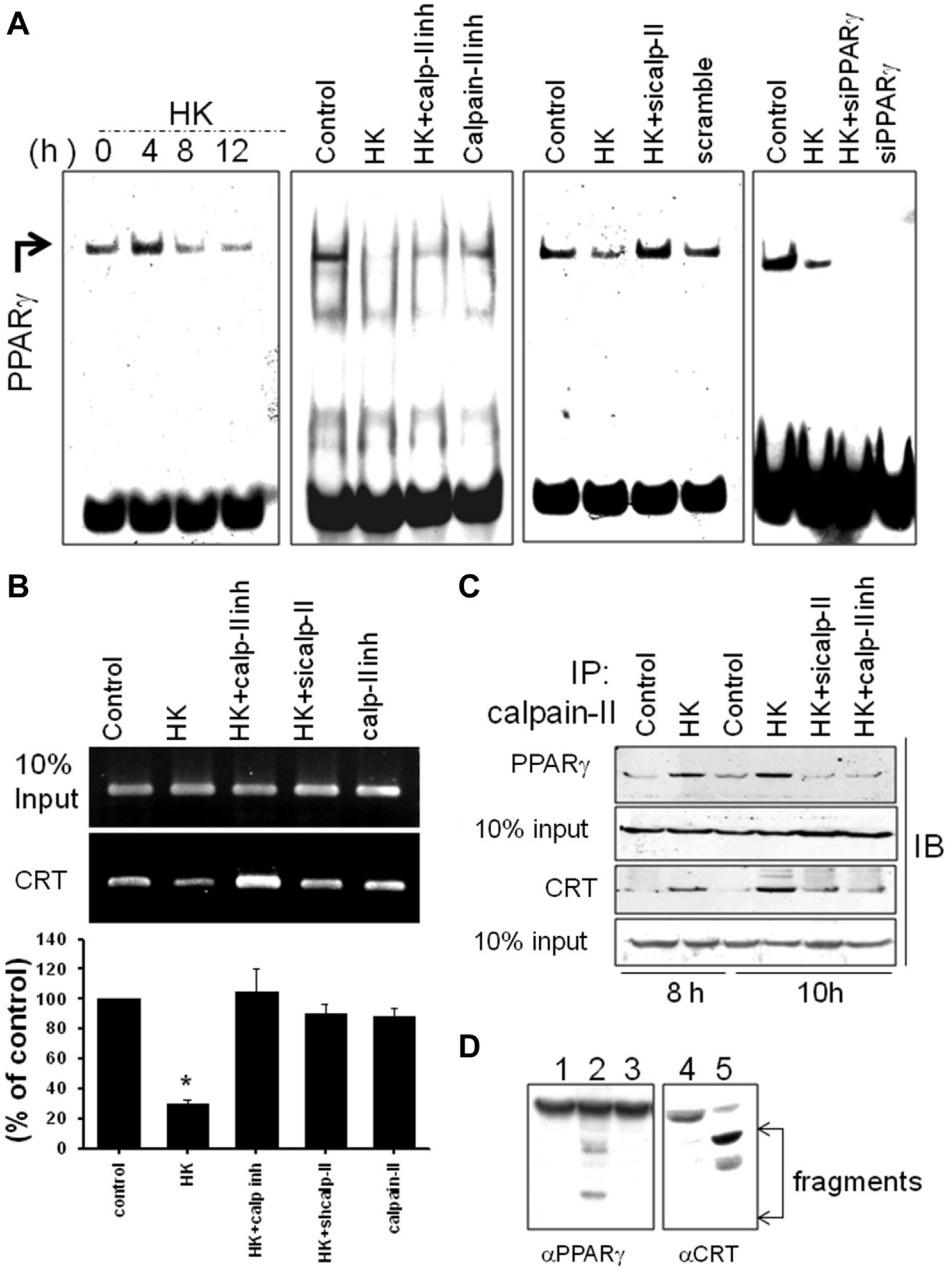

Figure 4 – Honokiol regulates PPARγ binds to CRT promoter sequences *in vitro*. The synthetic dsDNA representing PPARγ-binding sites in the promoter of CRT gene was examined by electrophoretic mobility shift assay (EMSA) using nuclear extracts of control or Honokiol following stimulation of cells. The unbound excess radiolabeled probe migrated out of the gel and is shown bottom. (A) Cancer cells AGS or MKN45 were treated with Honokiol at various time courses, and nuclear PPARγ DNA binding activity was analyzed by EMSA. Cancer cells were pretreated with calpain inhibitor or transfected with siRNA-Calpain-10, scrambled siRNA or siRNA-PPARγ followed by stimulation with Honokiol for 8 h. The results shown are representative of at least three independent experiments. Arrow indicates specific PPARγ sequences located on CRT promoter DNA binding. The PPARγ DNA binding labeled probe as indicated. All experiments were repeated at least three times. (B) PPARγ binds to the CRT promoter *in vivo*. ChIP assay was carried out with control, Honokiol or calpain inhibitor. After formaldehyde cross-linking, the PPARγ-binding DNA fragments were recovered by immunoprecipitation using PPARγ antibodies. Purified precipitates or input DNA was analyzed by PCR using primers specific for CRT promoters. The cross-links were reversed and the recovered DNA population was analyzed by PCR with primers designed for detecting CRT. An amplified PCR fragment is visible in the DNA immunoprecipitated with PPARγ antibody in CRT promoters. There is slim visible CRT band in the Honokiol-treated that could be reverse by Calpain inhibitors. PCR products were subjected to gel electrophoresis and visualized by ethidium bromide staining. 10% aliquot of the pre-cleared chromatin was taken as input. This experiment has been replicated at least four times with independently assay. All experiments were repeated at least four times. (C) AGS were treated with or without Honokiol as indicated for 10 h. Calpain-II was immunoprecipitated by anti-Calpain-II antibody from cell lysates and the immunoblot was probed with the antibodies for PPARγ or CRT. The results shown are representative of three independent experiments. (D) Proteolysis of PPARγ or CRT in the presence of Calpain-II enzymatic activity. Purified PPARγ or CRT was digested by the indicated

determine if activation of calpain-II was subsequent to ER stress, we explored whether the Honokiol and selective ER stress inducer tunicamycin (TUN), a protein N-glycosylation inhibitor, triggered activation of calpain-dependent ER stress signaling pathways by ERSE reporter assay. As shown in Figure 3A, Honokiol or TUN significantly induced ERSE reporter activity as indicated. Pharmacological calpain inhibitors or siRNA-calpain-II transfection indeed blocked the luciferase activity. Calpain-II recombinant protein served as the positive control. Promoter regulation in the CRT promoter-flanking region (−4700/−4670) containing the *cis*-acting elements PPARγ binding activity *in silico* was predicted. Our previous study showed that Honokiol inhibits gastric tumorigenesis via inhibition of PPAR-γ and COX-2-dependent signals (Liu et al., 2010a). Indeed, hyperactivation of transcriptional factor PPAR-γ stimulates the growth and metastatic potential in human cancer. Importantly, up-regulation of PPAR-γ and CRT expression in tumors were correlated with poor outcomes. Thus, in the present study we investigated PPAR-γ, CRT expression, and PPARγ activity. As shown in Figure 3B, Honokiol-induced calpain-II activity (data not shown) and protein expression reproducible previous results. Both calpain inhibitors and siRNA-calpain-II knockdown effectively blocked Honokiol-induced PPAR-γ, CRT protein depression. Moreover, Honokiol-suppressed PPAR-γ activity markedly reversed following exposure to calpain inhibitors and siRNA-calpain-II transfection (Figure 3C). Interference of PPAR-γ and recombinant protein calpain-II takes as the negative control. Scramble *per se* didn't any effect. These results suggest that Honokiol-induced calpain-II activation and ER stress control PPARγ and CRT expression.

3.4. *Honokiol regulates CRT expression via PPARγ*

The binding sites for PPARγ in the CRT promoter were predicted *in silico* and tested experimentally by EMSA and ChIP analyses. EMSA was performed to determine if the PPARγ protein directly bound to the CRT promoter region containing the PPARγ-binding sequence. Thus, a DNA probe spanning the −4700/−4670 region at the CRT promoter containing the canonical PPARγ consensus site was generated. As shown in Figure 4A, a band shift was detected for PPARγ expression in a time dependent manner when the −4700/−4670 probe was used in the assay. The binding of the PPARγ to the labeled probe could be competitively inhibited by 100-fold molar excess of unlabeled probes (data not shown). Furthermore, both pharmacological calpain inhibitor and siRNA-calpain-II transfection could effectively reverse the down-regulation of PPARγ DNA binding activity by Honokiol, supporting the hypothesis that PPARγ binds to CRT promoter region. Silencing PPARγ could also abolish the intense band and showed a greater effect than Honokiol-treated *per se*. A similar effect in the shift was reported for PPARγ knockdown itself. Importantly, an ER stress response element (ERSE) also adjacent to the TATA box is present in the CRT promoter of most species. Moreover, the application of ChIP using an anti-PPARγ antibody in MKN45 gastric cancer cells compared with pharmacological calpain inhibitors or si-calpain-II transfection cells showed that CRT promoter segments, a fragment spanning nucleotides −4700 to −4670 bp (−4700/−4670) containing the canonical consensus PPARγ-binding sequence bound most robustly to the PPARγ protein (Figure 4B). Immunoprecipitation of the PPARγ-containing DNA segment seemed to be specific, as ChIP using control human IgG instead of antibody did not reduce this fragment (data not shown). ChIP results revealed that PPARγ exhibited higher basal binding activities at predicted binding sites, and Honokiol potently reduced PPARγ binding to this site by calpain activity. In addition, Honokiol-decreased PPARγ binding activity could be reversed by pharmacological calpain inhibitors or gene silencing. These findings support the hypothesis that PPARγ directly regulates CRT promoter region. The relative quantification was evaluated by densitometry (Figure 4B, Lower panel). We next investigated the direct interaction of calpain-II and PPARγ. As shown in Figure 4C, Honokiol significantly enhances calpain-II/PPARγ interaction. Furthermore exposure to pharmacological calpain inhibitors or transfected si-RNA targeting for calpain-II significantly blocked the interaction. Unexpectedly, we found that calpain-II also interacted with CRT. That may be explained by the rapid down-regulation of CRT quickly down-regulation. Furthermore, we examined whether calpain-II cleaved PPARγ or CRT, by digesting concentrated PPARγ or CRT with recombinant calpain-II *in vitro* (Figure 4D). Incubation of PPARγ or CRT with recombinant calpain-II for 1 h at 30 °C led to the complete digestion of full-length PPARγ or CRT, as determined by *in vitro* cleavage assay. These results indicated that PPARγ or CRT could be cleaved and calpain-II and provide evidence that Honokiol-induced calpain activation thereby controlling PPARγ and CRT expression.

3.5. *CRT regulates cell invasion and EMT marker characteristics*

To determine whether CRT enhances human gastric cancer cells invasion and whether it modulates the actions of either carcinogen inducer MNNG or tumorigenesis inducer TGF-β, over-expressed plasmid CRT and siRNA-CRT were transfected into two human gastric cancer cells. In AGS and SCM-1 cells, Honokiol significantly suppressed cell invasion; combined with siRNA-CRT exhibited more suppression (data not shown). However, CRT over-expressed plasmid (pcDNA-CRT) overcame the effect and exerted a greater more invasion effect (Figure 5A). Moreover, MNNG (0.1 μM) or TGF-β1 (10 ng/ml) enhanced invasion, and targeting of CRT decreased invasion in AGS cells and thwarted MNNG- or TGF-β1-mediated invasion in both AGS and SCM-1 cells (Figure 5B). Combined with pcDNA-CRT was greater than that of either inducing alone (Figure 5C). Moreover, the combination of both MNNG- and TGF-β1 exerted a significantly greater stimulatory effect on invasion in cells with high CRT levels (data not shown),

concentrations of recombinant Calpain-II at 37 °C for 4 h in the presence of 0.5 mM $CaCl_2$. Samples were analyzed by 8% SDS-PAGE and stained with Coomassie blue. Data shown are from one experiment representative of at least three performed. Lane 1, Purified PPARγ protein; Lane 2, Purified PPARγ protein + recombinant Calpain-II, 0.1 U/ml; Lane 3, Purified PPARγ protein + Ca^{2+} 0.5 mM; Lane 4, Purified CRT protein; Lane Purified CRT protein + recombinant Calpain-II, 0.1 U/ml. The images are representative of at least five independent experiments.

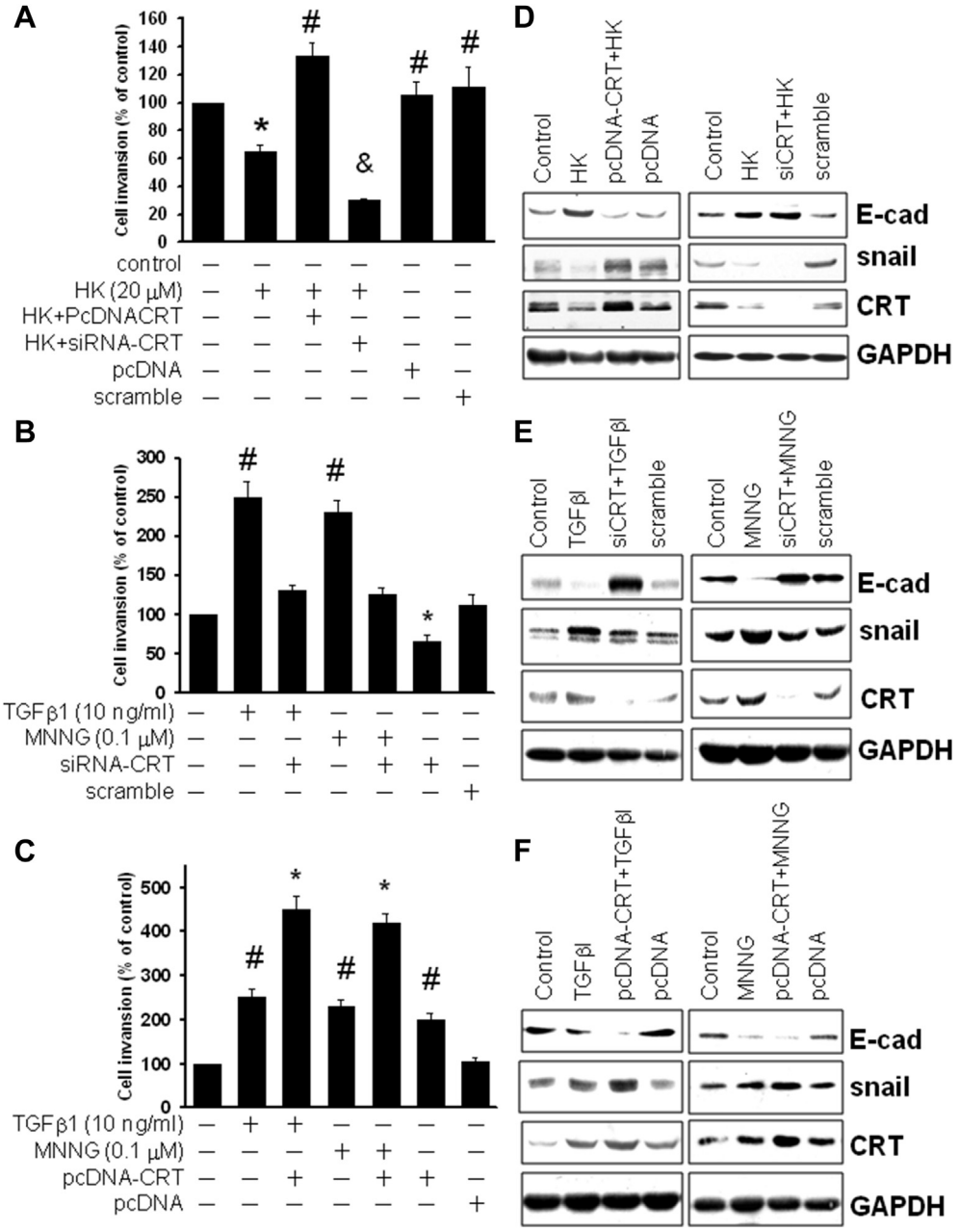

Figure 5 – CRT regulates cell invasion and EMT marker characteristics. Cancer was transfected with pcDNA3-CRT, pcDNA3 for overexpression CRT or siRNA-Calpain-II or scrambled siRNA for knockdown CRT protein, followed by stimulation with Honokiol, TGFβ1 or MNNG for 24 h. Cells were evaluated for invasion by Boyden's Transwell assay (A–C) or EMT markers were evaluated by Western blotting (D–F). Silencing CRT inhibited TGFβ1- or MNNG-induced cell invasion (B) and EMT marker E-cadherin (E-cad) (E) by CRT constraint in gastric cancer cells. Overexpression of CRT enhanced TGFβ1- or MNNG-induced cell invasion (C) and E-cad (F) by CRT augmentation in gastric cancer cells. AGS cells were treated with Honokiol for 24 h and whole-cell lysates were evaluated protein expression as indicated. The results shown are representative of at least five independent experiments. HK, Honokiol.

which is potentially important clinically given that CRT, under MNNG- and TGF-β were all over-expressed in gastric cancer cells.

We then examined whether CRT regulated mesenchymal (metastatic) properties were controlled by Honokiol. In addition, whether MNNG or TGF-β1 reduced epithelial cell signature and induced mesenchymal characteristics was not determined. We found that Honokiol significantly down-regulated Snail, CRT and up-regulated E-cadherin expression (Figure 5D). Additionally, knockdown with siRNA-CRT yielded results consistent with those of the Honokiol-treated findings (Figure 5E). Moreover, transfection of pcDNA-CRT was observed (Figure 5F). These results revealed that CRT regulates cell invasion and EMT marker characteristics.

3.6. CRT over-expression in carcinogen MNNG-induced tumor mass and knockdown of CRT inhibits in vivo metastasis of gastric tumors

To validate the contribution of CRT to gastric tumor production by carcinogens, an *in vivo* study was conducted in an MNNG-induced animal model using BL/6 and BALB/c mice (data not shown). MNNG (5 mg/kg, twice/weekly, i.p.) was used to test used for hypothesis as indicated at 1, 3, 6 months, that there would be high express tumor mass (Figure 6A–C), intense PCNA staining, and dense CRT levels. Additionally, after 3 months, five to eight animals in each group of the MNNG-induced animals were then randomly assigned to either with or without treatment with Honokiol (5 mg/kg Honokiol), and MNNG-induced tumor growth was periodically monitored for up to 6 months. As shown in Figure 6A–C, Honokiol substantially reduced the primary tumor mass, PNCA staining, compact CRT levels compared with those of the control tumor group. Moreover, we also confirmed that metastatic capacity was blocked by silencing CRT. Transfection with siRNA-CRT into MKN45 by intra-peritoneal injection was performed. As shown in Figure 6D–F, in the control group, tumors migrated to the abdominal, lung and liver, whereas siRNA-CRT groups showed less migration. Quantification of siRNA-CRT groups showed inhibition of metastatic organs of gastric tumor cells as shown in Figure 6E. These *in vivo* studies indicate significant inhibitions of tumor cell growth and metastasis. Thus, CRT exerts multiple deleterious actions in intestinal tissues, which include carcinogen MNNG-induced tumor mass signaling, decreased expression of metastasis by knockdown of CRT, thereby contributing to tumor proliferation and invasion.

4. Discussion

Our results support the hypothesis that CRT plays a key role in gastric cancer cell peritoneal dissemination and tumor growth, which can be modulated by Honokiol-induced ER stress. In addition, Honokiol confers immunogenicity by dictating CRT exposure inhibiting EMT. We showed that CRT is evidently over-expressed in both gastric tissues and gastric cancer cell lines. Pathologic investigation of human gastric cancer tissues demonstrated a significant correlation between CRT expression and clinical staging, as well as Tumor-Node-Metastasis classification of CRT. In the analysis of clinical samples of omentum or distal metastasis and lymph node metastasis clinical sample, we found that high CRT expression with markedly dense staining was a poor prognostic indicator in gastric patients. In animal experiments, carcinogen MNNG-induced tumorigenesis and CRT overexpression in tumor mass, that could be thwarted by Honokiol-treated. Additionally, down-regulation of CRT through siRNA inhibited the metastatic capability of CRT cells in the nude mice abdominal capacity, liver and lung, further demonstrating the potential function of CRT in promoting gastric cancer cell invasion. These data indicate that CRT detection could provide useful information about treatment strategy and prognosis, and could be provided histo-pathological diagnosis.

Calreticulin (CRT) as a multi-functional chaperone protein located in ER and is involved in a spectrum of cellular processes which have been implicated in calcium homeostasis, promotion of folding, oligomeric assembly, chaperoning to cell adhesion and malignant formation and progression (Wang et al., 2012b). CRT is known to be a characteristic expression pattern, which differentially expressed in various mammal cell types, suggesting the specific roles in each organ or tissue (Hayashida et al., 2006; Wang et al., 2012a). And previous studies have shown a contributing role for CRT in a range of different clinical cancers, such as gastric cancer, bladder cancer, pancreatic cancer and esophageal squamous cell carcinoma (Chen et al., 2009a, 2009b; Du et al., 2009; Lu et al., 2011; Obeid et al., 2007; Sheng et al., 2014; Suzuki et al., 2012; Wang et al., 2012a, 2013), although other studies demonstrated opposing findings, with down-regulation of CRT in neuroblastoma and prostate cancer (Alur et al., 2009; Hsu et al., 2005). In line with results reported by with Chen et al., CRT was shown to enhance angiogenesis, and facilitate proliferation and migration of gastric cancer cells, which is consistent with the association of CRT with MVD, tumor invasion, lymph node metastasis, and survival in gastric cancer patients (Chen et al., 2009a, 2009b). Indeed, our immunohistochemical studies are consistent with the aforementioned findings and demonstrated that increased CRT protein levels confer a worse clinical outcome in gastric cancer patients. Epithelial-to-mesenchymal transition (EMT) is critical during multiple stages of tumor development, facilitating cancer cell proliferation, angiogenesis, invasion and metastasis. Previous reported by Yasushi et al. showed that CRT is related to an EMT-like change of cellular phenotype and indicated overexpression of CRT repressed E-cadherin gene production via up-regulation of its repressor, Slug, via altered Ca^{2+} homeostasis in MDCK cells (Hayashida et al., 2006). In addition, Lu and colleagues found alteration of CRT expression levels might affect bladder cancer growth and metastasis *in vitro* and *in vivo* via Fak and Paxillin signaling (Lu et al., 2011). Kageyama et al. observed that higher expression of calreticulin was demonstrated in the urine of patients with bladder cancer and proposed calreticulin as a biomarker in bladder cancer (Kageyama et al., 2009). Recently, Sheng et al. also reported that IHC showed both CRT and p53 expression was significantly increased in pancreatic cancer, compared to that in paired non-cancerous pancreatic tissues (Sheng et al., 2014). Moreover, overexpression of CRT contributed to the development and progression of pancreatic cancer through MEK/ERK-signaling pathway but independently of p53. A study by Wang conducted an immunohistochemical analysis of CRT and PTP1B expression in ESCC tissues, and found a strong correlation (Wang et al., 2013). Although previous studies suggest that CRT possesses different functions, the roles of CRT in invasion, peritoneal dissemination and in regulating EMT progression remain poorly understood. In an *in silico* study, we found that CRT promoter regions −4700 to −4670 bp (−4700/−4670) containing the canonical consensus PPARγ-binding site. It is important to note that Honokiol-induced ER stress and activated specific calpain-II activity, but not specific calpain-I demonstrated in our previous report (Sheu et al., 2007). Honokiol could also inhibit PPARγ expression (Liu et al., 2010a). Moreover, we simultaneously

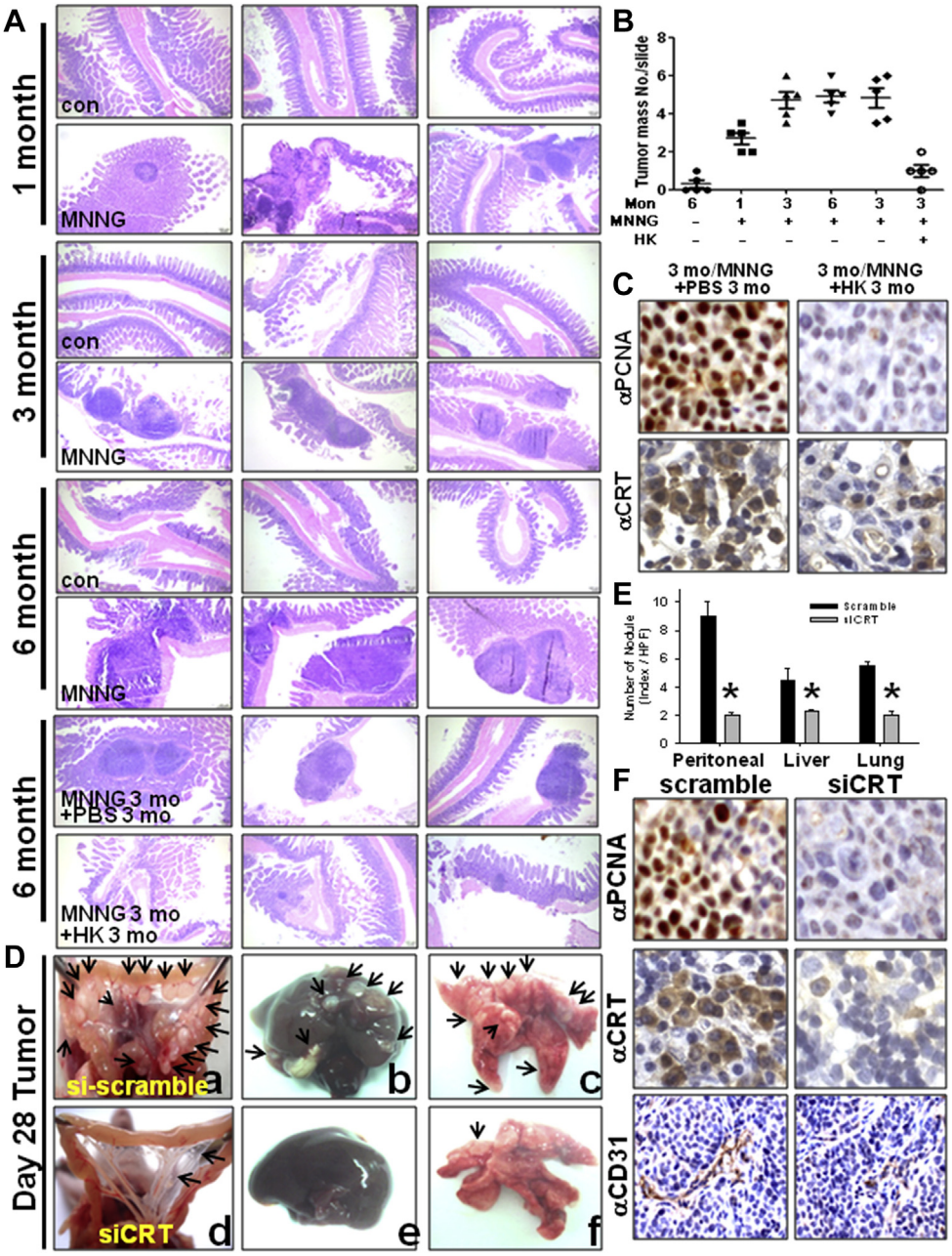

Figure 6 – CRT overexpression in carcinogen MNNG-induced tumor mass and knockdown CRT inhibits *in vivo* metastasis of gastric tumors. (A) Carcinogen MNNG-induced gastrointestinal tract tumor mass formation 1, 3, 6 months individually after intra-peritoneal injection (5 mg/kg) in administration to BL/6 mice. Another groups for therapy, which sustained for 3 months MNNG-induced and then derived two groups, then following with injected intraperitoneally with Honokiol (5 mg/kg/twice per week). Three months after Honokiol treatment, mice were sacrificed for tumor mass histology examination of the distribution of RT. (B) Microscopic hematoxylin and eosin staining appearance of the tumor growth of gastrointestinal tract of BL/6 mice after Carcinogen MNNG-induced tumor cells. At the end of the experiment, gastrointestinal tract along with the primary tumor from the control and Honokiol-treated mice were carefully excised and counted. The results are presented as a bar graph ($n = 5$). (C) Immunohistochemistry analysis of tumor mass stained with anti-PCNA (upper panel), anti-CRT (lower panel) of tumor burden. (D) Inhibition of gastric cancer growth favored *in vivo* by siRNA-CRT and siRNA-scramble. Transfections of siRNA-CRT and siRNA-scramble into MKN45 were performed using Lipofectin. Twenty-eight days after implantation in abdominal cavity administration to nu/nu mice, the animals were euthanized and their tumors were dissected. Distance of the secondary tumors that migrated from stomach was shown. Image photographic illustration of metastasize to peritoneal tumor, liver and lung. (E) Quantifications of numbers of metastases in different organs (counts/field) were calculated. All data are presented as mean ± SEM ($n = 7$). (F) Tissues analysis of tumor mass stained with anti-PCNA (upper panel), anti-CRT (lower panel) of tumor burden and CD31, an endothelial cell marker.

demonstrated that Honokiol-induced calpain-II activation and involve both PPARγ and CRT. Both of inhibition of calpain activity by calpain inhibitors and siRNA-calpain-II transfection dampen Honokiol-enhanced calpain-II activity, thwart phagocytosis effects (Supplementary Figure 2) and sustain longer at the membrane (Supplementary Figure 3). Furthermore, the present study showed that CRT inhibition by Honokiol dramatically suppressed tumor peritoneal dissemination and depressed mesenchymal characteristics. Overexpression of CRT promotes cell invasion. Other evidence demonstrated in animal model that CRT inhibition by Honokiol or gene targeting by siRNA-CRT causes a reduction in tumor mass and thwarts tumor growth within 4 weeks. These changes are in line with the results of PET/CT imaging detection and nodule counts in the present study. Furthermore, the specific function in carcinogen MNNG-induced tumor growth has been demonstrated to be markedly effective in the progression process until 6 months. Honokiol strictly reduced carcinogen MNNG-induced tumor promotion and progression which is consistent with anti-tumorigenesis function. Therefore, inhibition of high levels of CRT may offer new targets for therapeutic intervention to abolish tumor invasion and block EMT, eventually dampening peritoneal dissemination.

Initiating stimulus cancer cell death can be derived immunogenic or non-immunogenic. The immunogenic characteristics of immunogenic cell death (ICD) are mainly mediated by damage-associated molecular patterns (DAMPs), including ecto-CRT, secreted ATP and released high mobility group protein B1 (HMGB1), which are vital for the ICD of cancer cells. It is noteworthy that CRT is paradoxically found at the in the cytosol of living cancer which facilitates adhesion and exposure in dying cell surface that is involved in ICD, whereas promotes cellular phagocytic uptake. Gardai et al. demonstrated ecto-CRT and phosphatidylserine serves as a crucial recognition, initiates clearance of viable or ligand on apoptotic cells by UVB-light-induced (Gardai et al., 2005, 2006). A recent *in vitro* binding study indicated that nitrosative stress causes CRT externalization in association with PS on the inner leaflet of the plasma membrane, thereby allowing CRT to become exposed during apoptosis (Tyurina et al., 2007). Activation of ecto-CRT of cancer cell lines undergoing ICD in response to certain chemotherapeutics (such as mitoxantrone, oxaliplatin) also facilities their engulfment by dendritic cells, which leads to tumor antigen presentation and tumor-specific cytotoxic T lymphocyte (CTL) responses (Obeid et al., 2007; Panaretakis et al., 2009; Tesniere et al., 2010). Another recent study showed that the immunomodulatory functions of ecto-CRT reside in the amino terminal lectin domain, which can bind various glycosylated protein molecules exhibiting a fairly high binding affinity to various glycans, including carrageenan, alginic acids, and hyaluronic acids. That demonstrated that a recombinant N-terminal fragment of CRT (39-272) is a potent inducer of activation, macrophages maturation of B cells and can trigger Ig class switching by B cells without T cell help both *in vitro* and *in vivo* (Hong et al., 2010). In addition, the ability of these anticancer drugs and treatments to induce ICD was shown to rely on the induction of ER stress (Fucikova et al., 2014; Garg et al., 2012, 2014; Inoue and Tani, 2014; Kepp et al., 2013; Luo and Lee, 2013; Martins et al., 2011; Zitvogel et al., 2010). ER stress-inducing capabilities are mostly unexplored. Chemotherapy-induced CRT translocation pathway is dependent on PERK mediated phosphorylation of the translation initiation factor eIF2alpha, the secretory pathway and followed by partial activation of caspase-8 (but not caspase-3)-mediated B cell receptor associated protein 31 (BCAP31)-dependent conformational activation of BAX and BAK proteins has been proved by Panaretakis et al. (2009). Induction of CRT surface exposure by hypericin-PDT-induced ER stress is coordinated by a pathway that is different from the one induced by chemotherapeutics reported by Garg and Agostinis (2014). These novel findings may be speculated ER stress pathway plays an important part in inducing ICD by enabling pre-apoptotic surface exposure of CRT. Moreover, we demonstrated that Honokiol-induced ER stress and pre-apoptotic ecto-CRT might dock with cell membrane on the surface of cancer cells undergoing ICD in early stage. Subsequently, that follows the calpain-II activation cleavage CRT expression. Lastly, Honokiol dampens peritoneal dissemination. The present study demonstrates that the induction of ICD by the promising anticancer drug Honokiol was shown to depend on the induction of ER stress. In the present study, the precise molecular relationship between ER stress and the process of EMT in the induction of ICD by Honokiol warrants further study to better understand the relevance of these processes and the pathways that they regulate.

5. Conclusion

In view of the fact that peritoneal dissemination remains a highly challenging and mortal cancer, there is an urgent need for novel therapeutic agents, and thus it imperative that efficient biomarkers for gastric cancer diagnosis and prognosis be identified. In addition, it is necessary to determine to what extent level of CRT expression correlates with clinicopathological features and disease progression in gastric cancer whether it promotes gastric cancer cell invasion. Importantly, the quick and effective induction of CRT translocation by Honokiol was shown to be correlated with ER stress, which confers immunogenic response. A schematic diagram of a potential molecular mechanism of Honokiol targets is presented in Supplementary Figure 1 which suggests that Honokiol may have potential in the development of pharmaceutical drugs for ICD. Moreover, our findings revealed a novel role of Honokiol-induced ER stress and calpain-II activation that involves both PPARγ and CRT in the regulation of cancer cell migration and invasion. Carcinogen-MNNG induced CRT in tumorigenesis process that could be suppressed by Honokiol. Thus, Honokiol may have potential in the development of pharmaceutical drugs owing to its immunogenic effect as well as its ability to attenuate EMT progression, and peritoneal dissemination in intervention-dependent human diseases such as tumors.

Conflict of interest

The authors declare no conflict of interest.

Author contributions

W.-J.L., H.-C.P. and M.-L.S. designed research; D.-W.L., S.-M.W., and C.-S.C. performed research; H.-R.T., and C.-Y.L. contributed new reagents/analytic tools; Y.-C.P., Y.-J.J. T.-H.C. and M.-L.S. analyzed data; S.-H.L. and M.-L.S. wrote the paper.

Financial support

Ministry of Science and Technology; National Science Council, Taiwan (NSC102-2628-B-005-001-MY3); National Chung Hsing University, Taiwan (NCHU102-5037); Taichung Veterans General Hospital in Taiwan (TCVGH-1027314C; TCVGH-1037307C; TCVGH-1037308C; TCVGH-HK1038001).

Acknowledgments

CRT overexpressed plasmid from Genome Research Center, National Yang-Ming University.

Appendix A. Supplementary data

Supplementary data related to this article can be found at http://dx.doi.org/10.1016/j.molonc.2014.12.009.

REFERENCES

Alur, M., Nguyen, M.M., Eggener, S.E., Jiang, F., Dadras, S.S., Stern, J., Kimm, S., Roehl, K., Kozlowski, J., Pins, M., Michalak, M., Dhir, R., Wang, Z., 2009. Suppressive roles of calreticulin in prostate cancer growth and metastasis. Am. J. Pathol. 175, 882–890.

Chao, M.P., Majeti, R., Weissman, I.L., 2012. Programmed cell removal: a new obstacle in the road to developing cancer. Nat. Rev. Cancer 12, 58–67.

Chen, C.N., Chang, C.C., Su, T.E., Hsu, W.M., Jeng, Y.M., Ho, M.C., Hsieh, F.J., Lee, P.H., Kuo, M.L., Lee, H., Chang, K.J., 2009a. Identification of calreticulin as a prognosis marker and angiogenic regulator in human gastric cancer. Ann. Surg. Oncol. 16, 524–533.

Chen, C.N., Lin, J.J., Lee, H., Cheng, Y.M., Chang, K.J., Hsieh, F.J., Lai, H.S., Chang, C.C., Lee, P.H., 2009b. Association between color Doppler vascularity index, angiogenesis-related molecules, and clinical outcomes in gastric cancer. J. Surg. Oncol. 99, 402–408.

De, C.B., Berx, G., 2013. Regulatory networks defining EMT during cancer initiation and progression. Nat. Rev. Cancer 13, 97–110.

Du, X.L., Yang, H., Liu, S.G., Luo, M.L., Hao, J.J., Zhang, Y., Lin, D.C., Xu, X., Cai, Y., Zhan, Q.M., Wang, M.R., 2009. Calreticulin promotes cell motility and enhances resistance to anoikis through STAT3-CTTN-Akt pathway in esophageal squamous cell carcinoma. Oncogene 28, 3714–3722.

Eggleton, P., Llewellyn, D.H., 1999. Pathophysiological roles of calreticulin in autoimmune disease. Scand. J. Immunol. 49, 466–473.

Fried, L.E., Arbiser, J.L., 2009. Honokiol, a multifunctional antiangiogenic and antitumor agent. Antioxid. Redox Signal 11, 1139–1148.

Fucikova, J., Moserova, I., Truxova, I., Hermanova, I., Vancurova, I., Partlova, S., Fialova, A., Sojka, L., Cartron, P.F., Houska, M., Rob, L., Bartunkova, J., Spisek, R., 2014. High hydrostatic pressure induces immunogenic cell death in human tumor cells. Int. J. Cancer 135, 1165–1177.

Gardai, S.J., Bratton, D.L., Ogden, C.A., Henson, P.M., 2006. Recognition ligands on apoptotic cells: a perspective. J. Leukoc. Biol. 79, 896–903.

Gardai, S.J., McPhillips, K.A., Frasch, S.C., Janssen, W.J., Starefeldt, A., Murphy-Ullrich, J.E., Bratton, D.L., Oldenborg, P.A., Michalak, M., Henson, P.M., 2005. Cell-surface calreticulin initiates clearance of viable or apoptotic cells through trans-activation of LRP on the phagocyte. Cell 123, 321–334.

Garg, A.D., Agostinis, P., 2014. ER stress, autophagy and immunogenic cell death in photodynamic therapy-induced anti-cancer immune responses. Photochem. Photobiol. Sci. 13, 474–487.

Garg, A.D., Krysko, D.V., Verfaillie, T., Kaczmarek, A., Ferreira, G.B., Marysael, T., Rubio, N., Firczuk, M., Mathieu, C., Roebroek, A.J., Annaert, W., Golab, J., de, W.P., Vandenabeele, P., Agostinis, P., 2012. A novel pathway combining calreticulin exposure and ATP secretion in immunogenic cancer cell death. EMBO J. 31, 1062–1079.

Garg, A.D., Martin, S., Golab, J., Agostinis, P., 2014. Danger signalling during cancer cell death: origins, plasticity and regulation. Cell Death Differ. 21, 26–38.

Gherardi, E., Birchmeier, W., Birchmeier, C., Vande, W.G., 2012. Targeting MET in cancer: rationale and progress. Nat. Rev. Cancer 12, 89–103.

Hayashida, Y., Urata, Y., Muroi, E., Kono, T., Miyata, Y., Nomata, K., Kanetake, H., Kondo, T., Ihara, Y., 2006. Calreticulin represses E-cadherin gene expression in Madin-Darby canine kidney cells via Slug. J. Biol. Chem. 281, 32469–32484.

Hong, C., Qiu, X., Li, Y., Huang, Q., Zhong, Z., Zhang, Y., Liu, X., Sun, L., Lv, P., Gao, X.M., 2010. Functional analysis of recombinant calreticulin fragment 39-272: implications for immunobiological activities of calreticulin in health and disease. J. Immunol. 185, 4561–4569.

Hsu, W.M., Hsieh, F.J., Jeng, Y.M., Kuo, M.L., Chen, C.N., Lai, D.M., Hsieh, L.J., Wang, B.T., Tsao, P.N., Lee, H., Lin, M.T., Lai, H.S., Chen, W.J., 2005. Calreticulin expression in neuroblastoma – a novel independent prognostic factor. Ann. Oncol. 16, 314–321.

Inoue, H., Tani, K., 2014. Multimodal immunogenic cancer cell death as a consequence of anticancer cytotoxic treatments. Cell Death Differ. 21, 39–49.

Kageyama, S., Isono, T., Matsuda, S., Ushio, Y., Satomura, S., Terai, A., Arai, Y., Kawakita, M., Okada, Y., Yoshiki, T., 2009. Urinary calreticulin in the diagnosis of bladder urothelial carcinoma. Int. J. Urol. 16, 481–486.

Kepp, O., Menger, L., Vacchelli, E., Locher, C., Adjemian, S., Yamazaki, T., Martins, I., Sukkurwala, A.Q., Michaud, M., Senovilla, L., Galluzzi, L., Kroemer, G., Zitvogel, L., 2013. Crosstalk between ER stress and immunogenic cell death. Cytokine Growth Factor Rev. 24, 311–318.

Krysko, D.V., Garg, A.D., Kaczmarek, A., Krysko, O., Agostinis, P., Vandenabeele, P., 2012. Immunogenic cell death and DAMPs in cancer therapy. Nat. Rev. Cancer 12, 860–875.

Lee, W.J., Lan, K.H., Chou, C.T., Yi, Y.C., Chen, W.C., Pan, H.C., Peng, Y.C., Wang, K.B., Chen, Y.C., Chao, T.H., Tien, H.R., Sheu, W.H., Sheu, M.L., 2013. Tpl2 inhibitors thwart endothelial cell function in angiogenesis and peritoneal dissemination. Neoplasia 15, 1036–1048.

Lim, L., Michael, M., Mann, G.B., Leong, T., 2005. Adjuvant therapy in gastric cancer. J. Clin. Oncol. 23, 6220–6232.

Liu, S.H., Shen, C.C., Yi, Y.C., Tsai, J.J., Wang, C.C., Chueh, J.T., Lin, K.L., Lee, T.C., Pan, H.C., Sheu, M.L., 2010a. Honokiol inhibits gastric tumourigenesis by activation of 15-lipoxygenase-1 and consequent inhibition of peroxisome proliferator-activated receptor-γ and COX-2-dependent signals. Br. J. Pharmacol. 160, 1963–1972.

Liu, S.H., Wang, K.B., Lan, K.H., Lee, W.J., Pan, H.C., Wu, S.M., Peng, Y.C., Chen, Y.C., Shen, C.C., Cheng, H.C., Liao, K.K., Sheu, M.L., 2012. Calpain/SHP-1 interaction by Honokiol dampening peritoneal dissemination of gastric cancer in nu/nu mice. PLoS One 7, e43711.

Liu, S.H., Yang, C.N., Pan, H.C., Sung, Y.J., Liao, K.K., Chen, W.B., Lin, W.Z., Sheu, M.L., 2010b. IL-13 downregulates PPAR-γ/heme oxygenase-1 via ER stress-stimulated calpain activation: aggravation of activated microglia death. Cell Mol. Life Sci. 67, 1465–1476.

Lu, Y.C., Chen, C.N., Wang, B., Hsu, W.M., Chen, S.T., Chang, K.J., Chang, C.C., Lee, H., 2011. Changes in tumor growth and metastatic capacities of J82 human bladder cancer cells suppressed by down-regulation of calreticulin expression. Am. J. Pathol. 179, 1425–1433.

Luo, B., Lee, A.S., 2013. The critical roles of endoplasmic reticulum chaperones and unfolded protein response in tumorigenesis and anticancer therapies. Oncogene 32, 805–818.

Martins, I., Kepp, O., Schlemmer, F., Adjemian, S., Tailler, M., Shen, S., Michaud, M., Menger, L., Gdoura, A., Tajeddine, N., Tesniere, A., Zitvogel, L., Kroemer, G., 2011. Restoration of the immunogenicity of cisplatin-induced cancer cell death by endoplasmic reticulum stress. Oncogene 30, 1147–1158.

Obeid, M., Tesniere, A., Ghiringhelli, F., Fimia, G.M., Apetoh, L., Perfettini, J.L., Castedo, M., Mignot, G., Panaretakis, T., Casares, N., Metivier, D., Larochette, N., van, E.P., Ciccosanti, F., Piacentini, M., Zitvogel, L., Kroemer, G., 2007. Calreticulin exposure dictates the immunogenicity of cancer cell death. Nat. Med. 13, 54–61.

Pan, H.C., Lai, D.W., Lan, K.H., Shen, C.C., Wu, S.M., Chiu, C.S., Wang, K.B., Sheu, M.L., 2013a. Honokiol thwarts gastric tumor growth and peritoneal dissemination by inhibiting Tpl2 in an orthotopic model. Carcinogenesis 34, 2568–2579.

Pan, H.C., Yang, C.N., Hung, Y.W., Lee, W.J., Tien, H.R., Shen, C.C., Sheehan, J., Chou, C.T., Sheu, M.L., 2013b. Reciprocal modulation of C/EBP-alpha and C/EBP-beta by IL-13 in activated microglia prevents neuronal death. Eur. J. Immunol. 43, 2854–2865.

Panaretakis, T., Kepp, O., Brockmeier, U., Tesniere, A., Bjorklund, A.C., Chapman, D.C., Durchschlag, M., Joza, N., Pierron, G., van, E.P., Yuan, J., Zitvogel, L., Madeo, F., Williams, D.B., Kroemer, G., 2009. Mechanisms of pre-apoptotic calreticulin exposure in immunogenic cell death. EMBO J. 28, 578–590.

Raghavan, M., Wijeyesakere, S.J., Peters, L.R., Del, C.N., 2013. Calreticulin in the immune system: ins and outs. Trends Immunol. 34, 13–21.

Sheng, W., Chen, C., Dong, M., Zhou, J., Liu, Q., Dong, Q., Li, F., 2014. Overexpression of calreticulin contributes to the development and progression of pancreatic cancer. J. Cell Physiol. 229, 887–897.

Sheu, M.L., Liu, S.H., Lan, K.H., 2007. Honokiol induces calpain-mediated glucose-regulated protein-94 cleavage and apoptosis in human gastric cancer cells and reduces tumor growth. PLoS One 2, e1096.

Shin, N.R., Jeong, E.H., Choi, C.I., Moon, H.J., Kwon, C.H., Chu, I.S., Kim, G.H., Jeon, T.Y., Kim, D.H., Lee, J.H., Park, d.Y., 2012. Overexpression of Snail is associated with lymph node metastasis and poor prognosis in patients with gastric cancer. BMC Cancer 12, 521.

Suzuki, Y., Mimura, K., Yoshimoto, Y., Watanabe, M., Ohkubo, Y., Izawa, S., Murata, K., Fujii, H., Nakano, T., Kono, K., 2012. Immunogenic tumor cell death induced by chemoradiotherapy in patients with esophageal squamous cell carcinoma. Cancer Res. 72, 3967–3976.

Tesniere, A., Schlemmer, F., Boige, V., Kepp, O., Martins, I., Ghiringhelli, F., Aymeric, L., Michaud, M., Apetoh, L., Barault, L., Mendiboure, J., Pignon, J.P., Jooste, V., van, E.P., Ducreux, M., Zitvogel, L., Piard, F., Kroemer, G., 2010. Immunogenic death of colon cancer cells treated with oxaliplatin. Oncogene 29, 482–491.

Tsai, T.H., Chou, C.J., Cheng, F.C., Chen, C.F., 1994. Pharmacokinetics of Honokiol after intravenous administration in rats assessed using high-performance liquid chromatography. J. Chromatogr. B Biomed. Appl. 655, 41–45.

Tyurina, Y.Y., Basova, L.V., Konduru, N.V., Tyurin, V.A., Potapovich, A.I., Cai, P., Bayir, H., Stoyanovsky, D., Pitt, B.R., Shvedova, A.A., Fadeel, B., Kagan, V.E., 2007. Nitrosative stress inhibits the aminophospholipid translocase resulting in phosphatidylserine externalization and macrophage engulfment: implications for the resolution of inflammation. J. Biol. Chem. 282, 8498–8509.

Wang, H.T., Lee, H.I., Guo, J.H., Chen, S.H., Liao, Z.K., Huang, K.W., Torng, P.L., Hwang, L.H., 2012a. Calreticulin promotes tumor lymphocyte infiltration and enhances the antitumor effects of immunotherapy by up-regulating the endothelial expression of adhesion molecules. Int. J. Cancer 130, 2892–2902.

Wang, W.A., Groenendyk, J., Michalak, M., 2012b. Calreticulin signaling in health and disease. Int. J. Biochem. Cell Biol. 44, 842–846.

Wang, X.M., Shang, L., Zhang, Y., Hao, J.J., Shi, F., Luo, W., Zhang, T.T., Wang, B.S., Yang, Y., Liu, Z.H., Zhan, Q.M., Wang, M.R., 2013. PTP1B contributes to calreticulin-induced metastatic phenotypes in esophageal squamous cell carcinoma. Mol. Cancer Res. 11, 986–994.

Zamanian, M., Veerakumarasivam, A., Abdullah, S., Rosli, R., 2013. Calreticulin and cancer. Pathol. Oncol. Res. 19, 149–154.

Zitvogel, L., Kepp, O., Senovilla, L., Menger, L., Chaput, N., Kroemer, G., 2010. Immunogenic tumor cell death for optimal anticancer therapy: the calreticulin exposure pathway. Clin. Cancer Res. 16, 3100–3104.